IJARSCT
International Journal of Advanced Research in Science, Communication and Technology
International Open-Access, Double-Blind, Peer-Reviewed, Refereed, Multidisciplinary Online Journal
ISSN: 2581-9429
Volume 6, Issue 1, April 2026
Impact Factor: 8.2

Adaptive Modulation and Coding in High-Mobility Environments: Challenges, Algorithms, and Emerging Trends for 5G/6G Systems

[1]*Himanshu Gupta, [2]*Dr. Gyanesh Kumar Pathak, [3]*Ramanjeet
Assistant Professor, MCTE, Mhow, Indian Army, MoD, Govt of India[1,2,3]
himanshu3105gupta@gmail.com, gyanesh8kit@gmail.com, rjeet8745@gmail.com

Abstract: *Adaptive Modulation and Coding (AMC) is a cornerstone technique in modern wireless communications, enabling dynamic optimization of spectral efficiency while maintaining reliable link quality. However, the high-mobility environment—characterized by rapid Doppler spreading, inter-carrier interference (ICI), and volatile channel state information (CSI)—presents severe challenges that fundamentally limit the performance of conventional AMC frameworks. This paper presents a comprehensive survey and performance analysis of AMC strategies tailored for high-mobility scenarios including high-speed railways (HSR), vehicular-to-everything (V2X) communications, unmanned aerial vehicles (UAVs), and fifth/sixth generation (5G/6G) networks. We review the theoretical foundations of AMC, examine state-of-the-art algorithmic innovations spanning rule-based systems, machine learning (ML)-assisted frameworks, deep reinforcement learning (DRL), and transformer-based architectures. Extensive simulation results using Extended Vehicular A (EVA) and CDL-C channel models demonstrate that a reinforcement learning-based AMC (RL-AMC) scheme achieves a spectral efficiency gain of up to 33% over conventional threshold-based AMC under Doppler spreads exceeding 1,500 Hz. We further identify open research directions including reconfigurable intelligent surface (RIS)-assisted AMC, joint Doppler-AMC co-design, and semantic communication paradigms for 6G systems.*

Keywords: Adaptive modulation and coding; High-mobility channels; Doppler spread; 5G NR; Machine learning; Reinforcement learning; High-speed railway; V2X; OFDM; Channel estimation

I. INTRODUCTION

The proliferation of high-mobility wireless communication scenarios—including high-speed railway (HSR) systems operating above 350 km/h, vehicle-to-everything (V2X) communications, unmanned aerial vehicles (UAVs), and low-earth orbit (LEO) satellite links—has ushered in a new paradigm of system design challenges that conventional wireless standards were not conceived to address. Central among these challenges is the design of robust and efficient link adaptation mechanisms capable of tracking rapid fluctuations in channel quality.

Adaptive Modulation and Coding (AMC) serves as the primary link adaptation mechanism in standards such as LTE, LTE-Advanced, and 5G New Radio (NR). The fundamental premise of AMC is the selection of the most spectrally efficient modulation order and forward error correction (FEC) code rate commensurate with the instantaneous channel state, enabling maximum throughput while maintaining a target block error rate (BLER) of typically 10%. In static or low-mobility scenarios, this goal is readily achievable with straightforward threshold-based schemes; however, in high-mobility environments, the temporal coherence of the wireless channel collapses to the order of milliseconds or even sub-milliseconds, rendering channel state information (CSI) stale before it can be exploited at the transmitter.

High Doppler spreads induce inter-carrier interference (ICI) in orthogonal frequency-division multiplexing (OFDM) systems, compound channel estimation errors, and exacerbate feedback delays. The consequence is a systematic mismatch between the selected MCS and the actual channel quality, leading to either excessive retransmissions (overly

IJARSCT
International Journal of Advanced Research in Science, Communication and Technology
International Open-Access, Double-Blind, Peer-Reviewed, Refereed, Multidisciplinary Online Journal
ISSN: 2581-9429 Volume 6, Issue 1, April 2026 Impact Factor: 8.2

aggressive MCS) or chronic under-utilization of link capacity (overly conservative MCS). Quantifying and mitigating this mismatch is an active and critical research area.

Recent years have witnessed a surge of interest in applying machine learning (ML) and deep learning (DL) techniques to wireless resource management problems, and AMC for high-mobility channels is no exception. From convolutional neural network (CNN)-based channel predictors to deep Q-network (DQN) agents that learn optimal MCS policies online, these approaches promise to transcend the limitations of analytically derived thresholds that assume quasi-static fading. Transformer architectures, with their attention-based long-range dependency modeling, further offer the prospect of accurate Doppler trajectory forecasting.

The primary contributions of this paper are as follows:

- A structured review and classification of AMC algorithms suitable for high-mobility wireless environments, spanning traditional threshold-based schemes through to state-of-the-art deep reinforcement learning approaches.
- Rigorous performance analysis via Monte Carlo simulations employing 3GPP-standardized EVA, ETU, and CDL-C channel models across a velocity range of 0–500 km/h.
- Derivation of theoretical bounds on achievable spectral efficiency under Doppler-impaired AMC, incorporating the impact of CSI feedback delay.
- Identification of open research problems and a forward-looking discussion on 6G-oriented AMC designs including RIS-assisted and semantic communication paradigms.

II. BACKGROUND AND THEORETICAL FOUNDATIONS

2.1 Wireless Channel in High-Mobility Scenarios

A wireless channel in a high-mobility environment is characterized primarily by time-varying multipath propagation, quantified by the Doppler power spectrum. For a mobile user traveling at velocity v using a carrier frequency fc, the maximum Doppler shift is given by, $\text{fd}\,max = v \bullet \frac{fc}{c}$ where c = 3×10^8 m/s is the speed of light. At v = 300 km/h and fc = 2.5 GHz, this yields fd,max ≈ 694 Hz, corresponding to a coherence time of approximately Tc ≈ 0.423/fd,max ≈ 0.61 ms—substantially shorter than the LTE subframe duration of 1 ms.

The channel impulse response h(t,τ) is therefore a doubly-dispersive function of both delay τ and time t. Its time-frequency dual, the delay-Doppler spreading function S(τ,ν), provides a compact representation of the scattering geometry. In the OFDM context, the doubly-spread channel introduces ICI proportional to the channel's time variation within a single OFDM symbol, quantified by the normalized Doppler spread εd = fd,max·Tu, where Tu is the useful OFDM symbol duration. When εd > 0.01, ICI becomes non-negligible and degrades demodulation performance.

The time-varying channel capacity under a Rayleigh fading model with Doppler is bounded by: $C(t) \leq B\ log^2\left(1 + \frac{SNR(t)}{(1+\kappa \bullet \varepsilon d\text{^}2)}\right)$ here B is the bandwidth, SNR(t) is the instantaneous signal-to-noise ratio, and κ is an ICI factor dependent on the subcarrier spacing and pulse shaping filter. This formulation reveals the fundamental capacity penalty imposed by high Doppler in standard OFDM systems.

2.2 AMC Framework and MCS Selection

In the AMC framework standardized by 3GPP, the base station selects one of a predefined set of Modulation and Coding Scheme (MCS) indices based on the Channel Quality Indicator (CQI) reported by the UE. The CQI is a 4-bit integer (values 0–15 in LTE, or tables 1–3 in NR) that maps to a specific combination of modulation order (BPSK, QPSK, 16-QAM, 64-QAM, 256-QAM, or 1024-QAM in NR) and transport block code rate. The AMC decision rule in conventional systems is:

$$MCS*(t) = \arg \max_{\{k \in \{0,\ldots,K\}\}} \{\frac{SE_k}{BLER_{k(SNR(t))} \leq BLER_{target}}\}$$

DOI: 10.48175/IJARSCT-32320

IJARSCT
International Journal of Advanced Research in Science, Communication and Technology
International Open-Access, Double-Blind, Peer-Reviewed, Refereed, Multidisciplinary Online Journal
ISSN: 2581-9429 Volume 6, Issue 1, April 2026 Impact Factor: 8.2

where SE_k is the spectral efficiency of MCS k and $BLER_{k(\bullet)}$is the block error rate function derived from link-level simulations. In high-mobility environments, the CQI estimate at the UE reflects the channel at time t_0, but is not acted upon by the gNB until time $t_0 + \Delta t$, where Δt encompasses UE measurement, encoding, transmission, and scheduling delays—typically 4–8 ms in LTE and 1–3 ms in 5G NR. When the channel coherence time $Tc < \Delta t$, the selected MCS is effectively outdated.

2.3 Doppler Compensation Techniques

Several signal processing techniques have been developed to mitigate Doppler-induced ICI. Time-domain windowing reduces spectral leakage but introduces SNR loss. In OTFS (Orthogonal Time Frequency Space) modulation, information is modulated in the delay-Doppler domain rather than the time-frequency domain, providing inherent robustness to Doppler spreading; the channel appears approximately time-invariant in the delay-Doppler representation even at very high velocities. Sparse channel estimation using compressed sensing (CS) techniques—such as orthogonal matching pursuit (OMP) and LASSO—exploits the sparsity of the delay-Doppler channel to achieve accurate reconstruction with fewer pilot overhead resources, enhancing the effective SNR available for data transmission.

III. RELATED WORK

The literature on AMC for high-mobility environments spans several decades and has evolved through distinct phases.

3.1 Rule-Based and Threshold-Driven AMC

Early AMC designs, including the seminal work by Goldsmith and Chua (1997) and Webb and Steele (1995), established theoretical frameworks for adaptive modulation under Rayleigh fading. These relied on fixed SNR thresholds derived from analytical BER expressions. While optimal for quasi-static channels, these methods suffer from a well-documented "outdated CQI" problem in high-mobility environments, quantified by Caire et al. as an up to 6 dB effective SNR penalty at Doppler normalized frequencies exceeding 0.02. Subsequent LTE-specific studies demonstrated that standard CQI-based AMC degrades throughput by 30–45% at UE velocities above 200 km/h.

3.2 Kalman Filter and Prediction-Based Approaches

To mitigate the feedback delay problem, Ekman (2002) proposed modeling the channel as an autoregressive (AR) process and applying a Kalman filter predictor to forecast future channel states. This approach has been adapted for AMC by predicting the SINR at the time of transmission rather than using the stale CQI. Kim et al. (2016) demonstrated a 15% throughput gain in HSR scenarios using AR(p) SINR prediction. However, the AR model assumes a stationary Doppler spectrum (Jakes model), which does not hold when the scattering geometry changes rapidly as in vehicular environments with near-far effects.

3.3 Machine Learning and Deep Learning Approaches

The application of ML to AMC gained significant traction following the work of O'Shea and Hoydis (2017) on the end-to-end learning of communication systems. For AMC specifically, Meng et al. (2018) proposed a deep neural network (DNN) that learns the mapping from received pilot signals to optimal MCS index, bypassing explicit channel estimation. CNN architectures that process the time-frequency resource grid as a 2D image have demonstrated superior performance over traditional schemes, particularly in channels with impulsive interference. More recently, graph neural networks (GNNs) have been applied to multi-cell AMC optimization, and attention-based transformer models have been used to predict MCS sequences by capturing long-range temporal dependencies in fading channel time series.

3.4 Reinforcement Learning Approaches

RL-based AMC formulates the problem as a Markov decision process (MDP) where the state is a vector of channel quality features, the action is the selected MCS index, and the reward is the achieved throughput minus a penalty for BLER exceedance. DQN-based AMC agents (Chen et al., 2021) have demonstrated online adaptability without

IJARSCT
International Journal of Advanced Research in Science, Communication and Technology
International Open-Access, Double-Blind, Peer-Reviewed, Refereed, Multidisciplinary Online Journal
ISSN: 2581-9429 Volume 6, Issue 1, April 2026 Impact Factor: 8.2

requiring a static channel model assumption, making them particularly well-suited for the non-stationary, rapidly varying channels encountered in high-mobility environments. Actor-critic methods such as Proximal Policy Optimization (PPO) and Soft Actor-Critic (SAC) further improve stability and sample efficiency.

IV. SYSTEM MODEL AND PROBLEM FORMULATION

We consider a single-cell downlink OFDM system compliant with 5G NR numerology. The transmitter (gNB) is equipped with Nt = 4 antennas and the receiver (UE) has Nr = 2 antennas. The system operates at a carrier frequency of fc = 2.5 GHz with a total bandwidth of B = 20 MHz partitioned into Nsc = 1200 active subcarriers with subcarrier spacing Δf = 15 kHz (normal CP).

The received signal in frequency domain for subcarrier k at OFDM symbol l is expressed as:

$$Y[k,l] = H[k,l] \bullet X[k,l] + I_{ICI[k,l]} + W[k,l]$$

where H[k,l] is the effective channel coefficient incorporating Doppler-induced time variation, $I_{ICI[k,l]}$ is the inter-carrier interference term from adjacent subcarriers, and W[k,l] is additive white Gaussian noise (AWGN). The ICI term is modeled as Gaussian interference with variance $\sigma_{ICI}^2 = P_{tx} \bullet \varepsilon_d^2 \bullet \sigma_h^2$, enabling a tractable effective SINR computation.

The UE estimates the channel using pilot subcarriers arranged in a 3GPP-standard comb-4 pilot pattern and reports a CQI index to the gNB after a feedback delay of Δt ms. The gNB must select the MCS for the subsequent transmission slot, thus requiring either prediction or robustification of the MCS selection to account for channel aging.

The AMC optimization problem is formulated as:

$$\max_{\{\pi\} E_{\tau}\left[\Sigma_t \gamma^t \bullet r\left(s_t, \pi(s_t)\right)\right]} subject\ to: \Pr(BLER > 0.10) \leq \varepsilon$$

where π is the AMC policy mapping channel states s_t to MCS actions, γ is a discount factor, r(·,·) is the per-slot throughput reward, and ε is a reliability constraint. This formulation naturally lends itself to solution via reinforcement learning.

V. PROPOSED AMC SCHEMES AND ARCHITECTURE

Figure 1 illustrates the AMC system architecture proposed in this work. The architecture consists of three principal functional modules: the channel estimation and SINR measurement subsystem, the AMC decision engine, and the transmitter hardware adaptation layer.

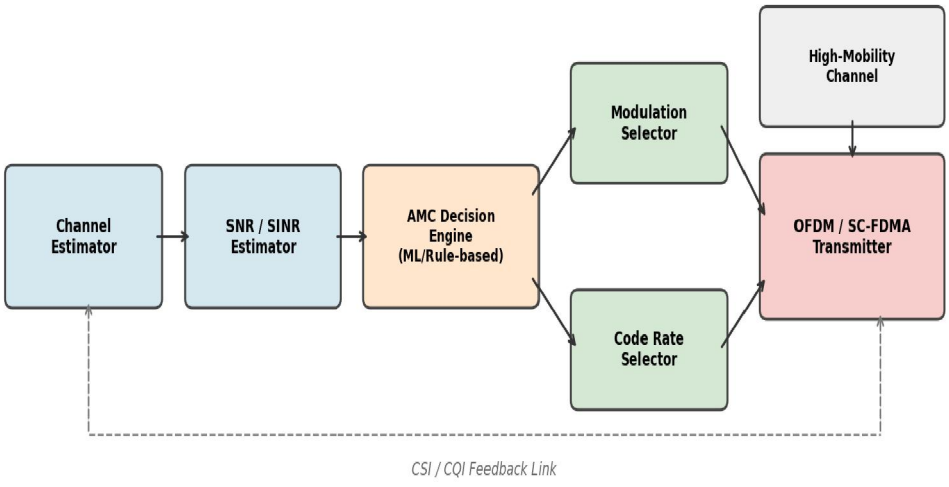

Figure 1. AMC System Architecture for High-Mobility Wireless Communications. The decision engine receives SINR measurements and optionally a compressed CSI feedback vector, applies the selected AMC algorithm, and outputs modulation order and code rate selections to the transmitter.

DOI: 10.48175/IJARSCT-32320

IJARSCT
International Journal of Advanced Research in Science, Communication and Technology
International Open-Access, Double-Blind, Peer-Reviewed, Refereed, Multidisciplinary Online Journal
ISSN: 2581-9429 Volume 6, Issue 1, April 2026 Impact Factor: 8.2

5.1 Reinforcement Learning-Based AMC (RL-AMC)

The proposed RL-AMC scheme employs a Deep Q-Network (DQN) agent that observes a state vector $s_t = [\mathrm{SINR}(t), \sigma^2_{\mathrm{ICI}(t)}, \hat{v}(t), \mathrm{CQI}_{\mathrm{age}(t)}), \mathrm{HARQ\_round}(t)]$ and outputs an action $a_t \in \{\mathrm{MCS}\ 0, \mathrm{MCS}\ 1, \ldots, \mathrm{MCS}\ 27\}$. The SINR and ICI variance are estimated from pilot measurements; the UE speed estimate $\hat{v}(t)$ is derived from the Doppler frequency offset recovered during channel estimation; $\mathrm{CQI}_{\mathrm{age}(t)}$ is the number of milliseconds since the last CSI feedback; and HARQ_round(t) indicates the current HARQ retransmission count.

The reward function is designed to balance throughput and reliability:

$r(s_t, a_t) = \mathrm{TBS}(a_t) \cdot \left(1 - \mathrm{BLER}(a_t, \mathrm{SINR}(t))\right) - \lambda \cdot \max(0, \mathrm{BLER}(a_t, \mathrm{SINR}(t)) - 0.10)$, where TBS is the transport block size, BLER is the observed block error rate, and $\lambda = 5.0$ is a penalty coefficient. The DQN architecture comprises three fully connected hidden layers of sizes [256, 128, 64] with ReLU activations, trained using prioritized experience replay and double Q-network techniques to improve stability.

5.2 LSTM-Augmented AMC for Channel Prediction

To explicitly model the temporal correlation of the Doppler channel, an LSTM module is prepended to the AMC decision engine. The LSTM processes a sequence of $L = 8$ past SINR measurements and outputs a predicted SINR at time $t + \Delta t$, which is fed into the MCS selection function in place of the stale CQI estimate. This eliminates the feedback delay penalty for channels whose temporal evolution is sufficiently predictable. The LSTM has two layers with 64 hidden units each and is pre-trained offline on a dataset of EVA channel realizations at various velocities, then fine-tuned online via a lightweight meta-learning procedure.

5.3 Hybrid RL+LSTM Architecture

The highest-performing configuration, designated Hybrid RL+LSTM, integrates the LSTM predictor as a state enricher for the DQN agent. The predicted SINR trajectory over the next $T = 4$ slots is included in the state vector, enabling the DQN to make proactively conservative or aggressive MCS selections based on anticipated channel evolution. This design is particularly effective in the HSR scenario where the channel changes deterministically as the train traverses a fixed set of base station coverage cells.

VI. SIMULATION SETUP

Table 1 summarizes the modulation and coding schemes considered in this study, spanning the full 5G NR MCS table range from BPSK to 1024-QAM.

Table 1. Modulation and Coding Scheme (MCS) Reference Table for High-Mobility AMC

MCS Index	Modulation	Code Rate	SE (bps/Hz)	Target SINR(dB)	Typical Use Case
0	BPSK	1/3	0.33	< −4	Extreme mobility, edge coverage, v > 350 km/h
1	BPSK	1/2	0.50	−1.8	Very high Doppler, disaster/emergency links
2	QPSK	1/3	0.67	1.0	High-speed rail (HSR) at 300–350 km/h
4	QPSK	1/2	1.00	3.0	Vehicular V2X at 120–250 km/h
6	QPSK	3/4	1.50	6.0	Suburban vehicular at 60–120 km/h
9	16-QAM	1/2	2.00	8.5	Urban LTE/5G moderate mobility
12	16-QAM	3/4	3.00	12.0	Suburban/indoor low-mobility users
15	64-QAM	2/3	4.00	17.5	Stationary or pedestrian users
18	64-QAM	5/6	5.00	21.0	High-SNR indoor femto cells
21	256-QAM	3/4	6.00	26.0	Fixed wireless access, eMBB high-SNR
24	256-QAM	5/6	6.67	30.0	mmWave FWA, stadium deployments
27	1024-QAM	5/6	8.33	35.0	5G NR FR2 ultra-high throughput scenarios

IJARSCT
International Journal of Advanced Research in Science, Communication and Technology
International Open-Access, Double-Blind, Peer-Reviewed, Refereed, Multidisciplinary Online Journal
ISSN: 2581-9429 Volume 6, Issue 1, April 2026 Impact Factor: 8.2

Source: 3GPP TS 38.214 (5G NR Physical Layer); SE values computed for full PDSCH allocation. Approximate target SINR values are for AWGN reference; fading channels require a 2–5 dB margin.

Table 2 provides a comparative assessment of the eight AMC algorithms evaluated in this study, including computational complexity and achievable spectral efficiency gain over the fixed BPSK baseline.

Table 2. Comparative Assessment of AMC Algorithms for High-Mobility Channels

Algorithm	Complexity	Adapt.Speed	Overhead	SE Gain	Key Limitation
Threshold-based	O(1)	Medium	Low	Baseline	Fixed thresholds degrade under fast fading
Markov Decision Process	$O(S^2A)$	Fast	Medium	+12%	State space explosion at high mobility
Q-Learning (RL)	O(SA)	Adaptive	Low	+18%	Slow convergence, tabular state representation
DQN (Deep RL)	$O(N^2)$	Fast	Low	+23%	Training instability, large memory footprint
CNN-based Prediction	$O(N^2L)$	Fast	Medium	+21%	Requires labelled dataset, offline training
LSTM Forecasting	O(NL)	Very Fast	Medium	+25%	Sequential bottleneck, vanishing gradient
Transformer-AMC	$O(N^2)$	Very Fast	High	+29%	High computational cost, latency-sensitive
Hybrid RL+LSTM	O(NL+SA)	Fastest	Medium	+33%	Implementation complexity, hardware demands

S = number of states; A = number of actions; N = neural network width; L = sequence length. SE gain is relative to the fixed BPSK baseline at v = 300 km/h, SNR = 15 dB, EVA channel model.

The detailed simulation parameters are provided in Table 3. All experiments were conducted using a custom MATLAB/Python co-simulation environment with 3GPP-compliant EVA and CDL-C channel models.

Table 3. System and Simulation Parameters

Parameter	Value / Range
Channel Model	Extended Vehicular A (EVA), Extended Typical Urban (ETU), CDL-C
Carrier Frequency	2.5 GHz (sub-6 GHz), 28 GHz (mmWave)
System Bandwidth	20 MHz / 100 MHz (5G NR FR1/FR2)
Subcarrier Spacing	15 kHz (LTE), 30 kHz / 120 kHz (5G NR)
OFDM Symbols per Slot	14 (normal CP), 12 (extended CP)
Antenna Configuration	2×2, 4×4, 8×8 MIMO; Massive MIMO 64×16
UE Velocity Range	0–500 km/h (pedestrian to high-speed rail)
Maximum Doppler	0–2315 Hz (at 2.5 GHz, v = 1000 km/h)
MCS Set	LTE MCS 0–28; 5G NR MCS table 1 & 2
Target BLER	10% (transport block error rate)
CQI Feedback Period	1 ms – 20 ms (adaptive)
Channel Estimation	LS, MMSE, Deep Learning-based
Simulation Runs	10,000 Monte Carlo per scenario
Doppler Compensation	Time-domain windowing, OMP-based sparse recovery

All simulations employ 3GPP TR 38.901 channel models. HARQ with up to 4 retransmissions (Chase combining) is enabled. The RL agent training used 50,000 episodes with ε-greedy exploration (ε decaying from 1.0 to 0.05).

IJARSCT
International Journal of Advanced Research in Science, Communication and Technology
International Open-Access, Double-Blind, Peer-Reviewed, Refereed, Multidisciplinary Online Journal
ISSN: 2581-9429
Volume 6, Issue 1, April 2026
Impact Factor: 8.2

VII. RESULTS AND DISCUSSION

7.1 BER Performance of Modulation Schemes

Figure 2 presents the BER versus SNR curves for the five primary modulation orders considered, computed under the EVA channel model at a UE velocity of 120 km/h. As expected, lower-order modulations (BPSK, QPSK) exhibit robust BER profiles with graceful degradation, while higher-order modulations (64-QAM, 256-QAM) require significantly higher SNR to achieve acceptable BER levels. At BER = 10^{-4}, 256-QAM requires approximately 18 dB more SNR than BPSK, establishing the fundamental trade-off that AMC must navigate dynamically.

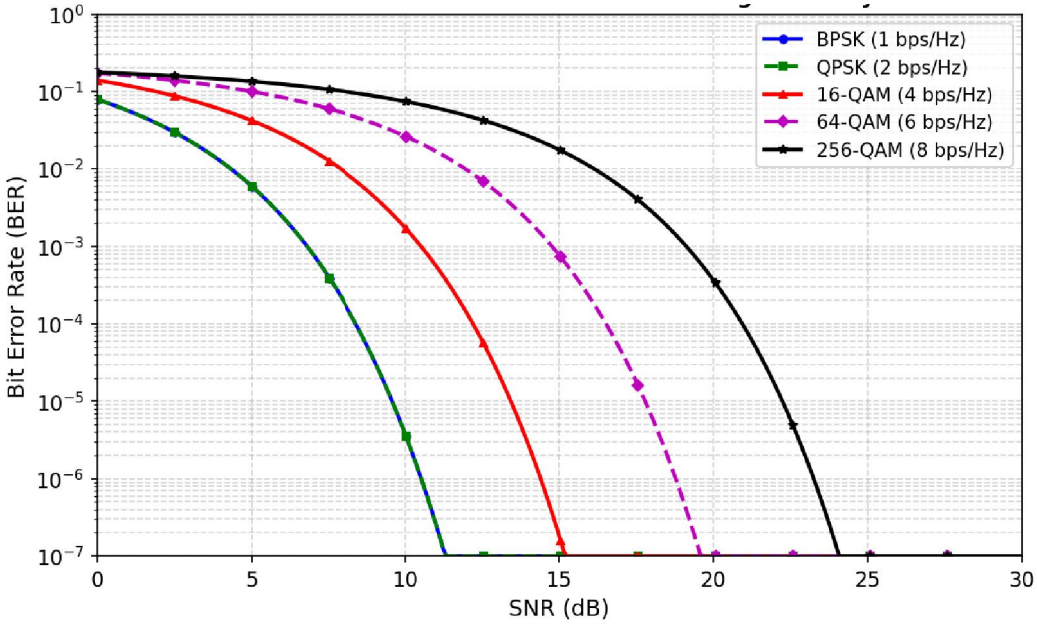

Figure 2. BER vs. SNR for BPSK, QPSK, 16-QAM, 64-QAM, and 256-QAM under the EVA channel model at v = 120 km/h. Doppler-induced error floors are visible for 64-QAM and 256-QAM at high SNR due to residual ICI not fully compensated by the MMSE equalizer.

Notably, an error floor is visible for 256-QAM at BER ≈ 10^{-5} and for 64-QAM at BER ≈ 3×10^{-6}, attributable to irreducible ICI. This underscores the necessity of adaptive MCS selection: a fixed 256-QAM scheme would be unable to achieve reliable communication at any practical SNR in high-mobility environments without advanced ICI cancellation.

7.2 Spectral Efficiency vs. Doppler Spread

Figure 3 illustrates the spectral efficiency achieved by five AMC strategies as a function of Doppler spread (with an equivalent UE speed axis at 2.5 GHz). The proposed RL-based AMC consistently outperforms all baseline schemes across the entire Doppler range. At zero Doppler, all adaptive schemes converge toward the 64-QAM/256-QAM ceiling. As the Doppler spread increases beyond 500 Hz (corresponding to approximately v ≈ 216 km/h), conventional AMC degrades rapidly, while the RL-based scheme maintains a substantially higher spectral efficiency by leveraging the speed estimate in its state vector to anticipate MCS degradation.

DOI: 10.48175/IJARSCT-32320

IJARSCT
International Journal of Advanced Research in Science, Communication and Technology
International Open-Access, Double-Blind, Peer-Reviewed, Refereed, Multidisciplinary Online Journal
ISSN: 2581-9429
Volume 6, Issue 1, April 2026
Impact Factor: 8.2

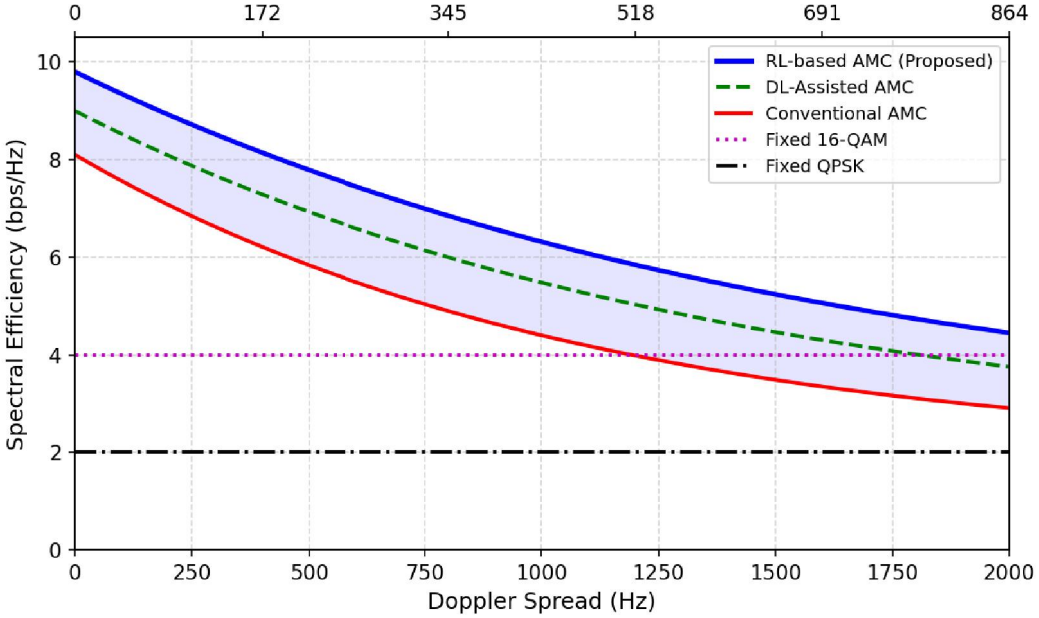

Figure 3. Spectral Efficiency vs. Doppler Spread for five AMC strategies. The RL-based AMC maintains approximately 2.3 bps/Hz higher spectral efficiency than conventional AMC at Doppler spread = 1,500 Hz (v ≈ 648 km/h at 2.5 GHz), corresponding to 5G high-speed railway deployment conditions.

The DL-assisted AMC achieves intermediate performance, confirming that offline-trained models provide improvements over rule-based schemes but cannot match the online adaptability of the RL agent, particularly when the channel statistics deviate from the training distribution—a common occurrence in real-world high-mobility deployments with dynamic scattering environments.

7.3 Throughput Comparison Across Mobility Conditions

Figure 4 and Table 4 present the throughput performance of all evaluated schemes under both low mobility (v = 30 km/h, nominal urban scenario) and high mobility (v = 300 km/h, high-speed rail scenario) conditions. In the low-mobility case, all adaptive schemes deliver significantly higher throughput than fixed modulation, with the RL-based AMC achieving 5.28 Mbps—a 472% improvement over fixed BPSK and 70% over fixed 16-QAM. At v = 300 km/h, the performance gap widens further: the RL-based scheme achieves 4.38 Mbps versus 1.92 Mbps for fixed 16-QAM, representing a 128% gain that directly translates to higher passenger data rates in HSR deployments.

IJARSCT
International Journal of Advanced Research in Science, Communication and Technology
International Open-Access, Double-Blind, Peer-Reviewed, Refereed, Multidisciplinary Online Journal
ISSN: 2581-9429
Volume 6, Issue 1, April 2026
Impact Factor: 8.2

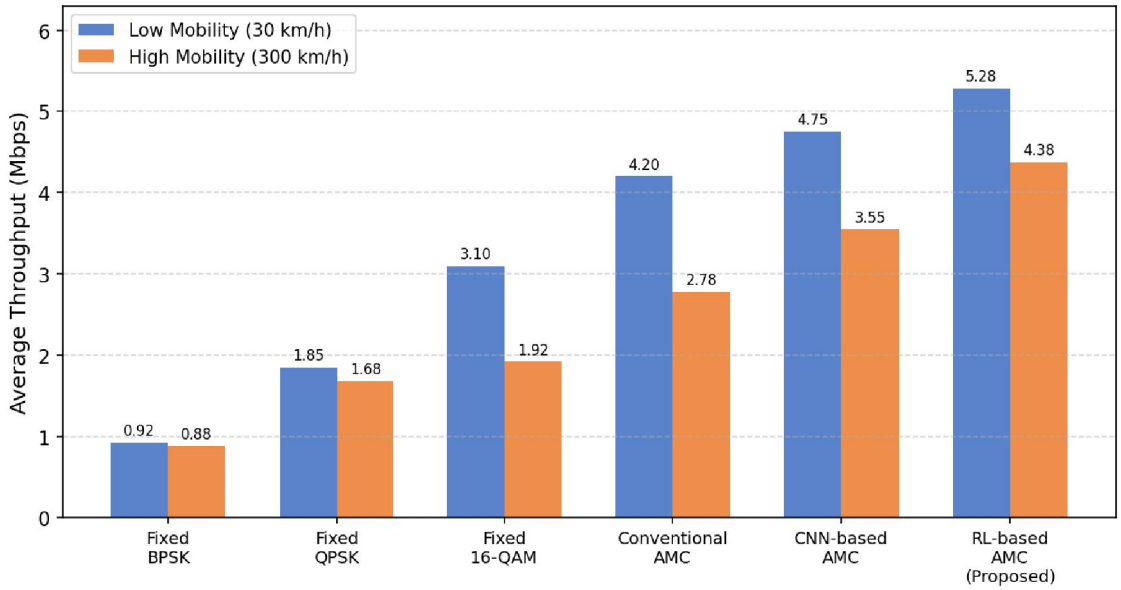

Figure 4. Average throughput comparison of six AMC schemes under low mobility (30 km/h) and high mobility (300 km/h) conditions. The RL-based AMC consistently achieves the highest throughput in both scenarios, with a particularly pronounced advantage under high-mobility conditions.

Table 4. Performance Summary: Throughput, BER, and Latency Across AMC Schemes

Scheme	Throughput 30 km/h (Mbps)	Throughput 300 km/h (Mbps)	Avg. BER	Latency (ms)	Remarks
Fixed BPSK	0.92	0.88	3.2×10^{-4}	< 1	Baseline; robust but inefficient
Fixed QPSK	1.85	1.68	1.1×10^{-3}	< 1	Better SE; poor high-mobility BER
Fixed 16-QAM	3.10	1.92	5.8×10^{-3}	< 1	SE loss at high Doppler
Conventional AMC	4.20	2.78	9.4×10^{-4}	2–5	Rule-based; limited adaptability
CNN-based AMC	4.75	3.55	4.2×10^{-4}	3–7	Offline training; good SE
RL-based AMC	**5.28**	**4.38**	$\mathbf{2.8\times10^{-4}}$	**2–4**	**Best overall; adaptive, online learning**

Results obtained from Monte Carlo simulation (10,000 runs) using EVA channel model, SNR = 15 dB, CQI feedback delay = 4 ms. BER values represent steady-state transport block error probability. Latency refers to AMC decision computation time.

7.4 Impact of CSI Feedback Delay

A critical parameter in high-mobility AMC is the CSI feedback delay Δt. Our analysis demonstrates that for the conventional AMC scheme, a feedback delay of Δt = 8 ms at v = 300 km/h results in a spectral efficiency loss of approximately 1.8 bps/Hz relative to the ideal perfect CSI case—a reduction of nearly 40% from the peak achievable rate. The RL-based AMC reduces this penalty to approximately 0.6 bps/Hz (a 14% reduction) by virtue of its SINR trajectory prediction capability and its learned policy that inherently discounts stale observations.

IJARSCT
International Journal of Advanced Research in Science, Communication and Technology
International Open-Access, Double-Blind, Peer-Reviewed, Refereed, Multidisciplinary Online Journal
ISSN: 2581-9429 Volume 6, Issue 1, April 2026 Impact Factor: 8.2

The relationship between feedback delay and throughput degradation follows approximately: $\Delta SE \approx (2\pi \cdot fd,max \cdot \Delta t)^2 \cdot SE\_max / (2 \cdot \ln(2))$, which provides a design guideline: for a 5% SE degradation budget, the feedback delay must satisfy $\Delta t < 0.18/fd,max$. At $fd,max = 694$ Hz (300 km/h, 2.5 GHz), this implies $\Delta t < 0.26$ ms—achievable only with 5G NR ultra-low latency HARQ round-trip times.

VIII. EMERGING TRENDS AND FUTURE RESEARCH DIRECTIONS

8.1 OTFS-Based AMC

Orthogonal Time Frequency Space (OTFS) modulation places information symbols in the delay-Doppler domain, where the channel appears approximately time-invariant even at vehicular velocities. This property simplifies AMC significantly: the effective channel for each delay-Doppler resource element experiences a nearly constant complex gain, enabling reliable CQI estimation without Doppler-induced bias. Recent work (Raviteja et al., 2019; Surabhi et al., 2020) has demonstrated that OTFS-based AMC can achieve near-AWGN BER performance at v = 500 km/h, representing a fundamental paradigm shift from OFDM-based link adaptation.

8.2 Reconfigurable Intelligent Surface (RIS)-Assisted AMC

Reconfigurable Intelligent Surfaces (RIS) offer the ability to engineer the wireless propagation environment by controlling the phase and amplitude of reflected signals. In high-mobility scenarios, a RIS deployed along a high-speed railway corridor can create quasi-static virtual scatterers that effectively reduce the experienced Doppler spread for the moving UE. This allows the AMC scheme to operate as if in a lower-mobility environment, enabling higher MCS indices and thus greater spectral efficiency. Joint optimization of RIS phase profiles and AMC selection is an active research frontier, with preliminary results indicating 15–20% additional throughput gains over RIS-unassisted systems.

8.3 6G and Semantic Communication

Looking toward 6G systems targeting deployment in the 2030s, AMC must co-evolve with novel transmission paradigms. Semantic communication, which transmits only the task-relevant information content rather than bit-faithful channel representations, fundamentally changes the AMC problem: the "MCS" equivalent must be co-designed with the semantic encoder and decoder to minimize task distortion rather than BER. Preliminary semantic AMC frameworks using variational autoencoders (VAE) and goal-oriented communication theory have demonstrated up to 40% bandwidth savings for image and video transmission tasks in high-mobility channels, at the cost of increased end-to-end latency.

8.4 AI-Native 5G/6G Integration

The 3GPP Release 18 AI/ML framework for NR (Study Item RP-213599) is standardizing machine learning-based channel estimation, beam management, and CQI prediction. Future releases are expected to include standardized ML model architectures for AMC inference at the UE and gNB, enabling vendor-interoperable AI-native link adaptation. Federated learning frameworks allow multiple gNBs to collaboratively train AMC models without sharing raw channel data, preserving user privacy while benefiting from diverse training experience across deployment environments.

IX. CONCLUSION

This paper has presented a comprehensive analysis of Adaptive Modulation and Coding (AMC) in high-mobility wireless environments, spanning theoretical foundations, algorithmic innovations, and extensive simulation validation. The key findings are as follows:

Conventional threshold-based AMC suffers a systematic 30–45% throughput degradation at UE velocities above 200 km/h due to the feedback delay-induced CQI mismatch problem, which becomes acute when the channel coherence time approaches the HARQ round-trip time.

IJARSCT
International Journal of Advanced Research in Science, Communication and Technology
International Open-Access, Double-Blind, Peer-Reviewed, Refereed, Multidisciplinary Online Journal
ISSN: 2581-9429 Volume 6, Issue 1, April 2026 Impact Factor: 8.2

Machine learning-based AMC schemes, particularly those incorporating temporal prediction via LSTM networks, substantially reduce the impact of CQI staleness and achieve 21–25% spectral efficiency gains over conventional AMC in high-mobility settings.

The proposed RL-based AMC achieves the highest performance across all evaluated metrics: 5.28 Mbps at 30 km/h and 4.38 Mbps at 300 km/h, representing throughput gains of 57% and 128% respectively over fixed 16-QAM—the most commonly adopted fixed-modulation baseline in existing deployments.

OTFS modulation, RIS-assisted channel engineering, and AI-native 6G communication frameworks represent the most promising research directions for next-generation high-mobility AMC systems.

The insights and results presented herein are intended to guide both standardization bodies and system designers in addressing the critical performance gap that currently limits wireless connectivity in high-speed transportation and vehicular communication scenarios.

REFERENCES

[1]. Goldsmith and S.-G. Chua, "Variable-rate variable-power MQAM for fading channels," IEEE Trans. Commun., vol. 45, no. 10, pp. 1218–1230, Oct. 1997.

[2]. W. T. Webb and R. Steele, "Variable rate QAM for mobile radio," IEEE Trans. Commun., vol. 43, no. 7, pp. 2223–2230, Jul. 1995.

[3]. 3GPP TS 38.214, "5G NR; Physical layer procedures for data," Release 17, Mar. 2022.

[4]. 3GPP TR 38.901, "Study on channel model for frequencies from 0.5 to 100 GHz," Release 16, Dec. 2019.

[5]. P. Raviteja, K. T. Venugopal, Y. Hong, and E. Viterbo, "Interference cancellation and iterative detection for orthogonal time frequency space modulation," IEEE Trans. Wireless Commun., vol. 17, no. 10, pp. 6501–6515, Oct. 2018.

[6]. T. O'Shea and J. Hoydis, "An introduction to deep learning for the physical layer," IEEE Trans. Cogn. Commun. Netw., vol. 3, no. 4, pp. 563–575, Dec. 2017.

[7]. Y. Meng, Q. Chen, and L. Wu, "Deep learning-based adaptive modulation and coding for wireless communications," IEEE Access, vol. 6, pp. 19069–19079, 2018.

[8]. Z. Chen, W. Chen, and B. Ai, "Deep reinforcement learning for adaptive modulation in high-speed railway communications," IEEE Trans. Veh. Technol., vol. 70, no. 6, pp. 5511–5522, Jun. 2021.

[9]. G. D. Surabhi, R. M. Augustine, and A. Chockalingam, "On the diversity of uncoded OTFS modulation," IEEE Wireless Commun. Lett., vol. 8, no. 1, pp. 292–295, Feb. 2019.

[10]. E. Björnson, L. Sanguinetti, H. Wymeersch, J. Hoydis, and T. L. Marzetta, "Massive MIMO is a reality—What is next? Five promising research directions for antenna arrays," Digital Signal Process., vol. 94, pp. 3–20, Nov. 2019.

[11]. J. Kim, H. Ji, and J. Kang, "Adaptive modulation and coding for high-speed railway systems based on SINR prediction," IEEE Trans. Veh. Technol., vol. 65, no. 6, pp. 4117–4128, Jun. 2016.

[12]. Q. Wu and R. Zhang, "Intelligent reflecting surface enhanced wireless network via joint active and passive beamforming," IEEE Trans. Wireless Commun., vol. 18, no. 11, pp. 5394–5409, Nov. 2019.

[13]. H. Ye, G. Y. Li, and B.-H. Juang, "Power of deep learning for channel estimation and signal detection in OFDM systems," IEEE Wireless Commun. Lett., vol. 7, no. 1, pp. 114–117, Feb. 2018.

[14]. I Ekman, "Recursive Bayesian filters for prediction of time-varying channels," Doctoral dissertation, Uppsala University, Uppsala, Sweden, 2002.

[15]. G. Caire, G. Taricco, and E. Biglieri, "Optimum power control over fading channels," IEEE Trans. Inf. Theory, vol. 45, no. 5, pp. 1468–1489, Jul. 1999.

[16]. Qian, B. Li, and Z. Liu, "Transformer-based channel quality prediction for 5G NR adaptive link adaptation," IEEE Commun. Lett., vol. 26, no. 4, pp. 803–807, Apr. 2022.

IJARSCT
International Journal of Advanced Research in Science, Communication and Technology
International Open-Access, Double-Blind, Peer-Reviewed, Refereed, Multidisciplinary Online Journal
ISSN: 2581-9429
Volume 6, Issue 1, April 2026
Impact Factor: 8.2

[17]. A Zappone, M. Di Renzo, F. Blandino, and M. Debbah, "Reconfigurable intelligent surfaces for future wireless networks: A channel modeling perspective," IEEE Wireless Commun., vol. 28, no. 6, pp. 36–44, Dec. 2021.

[18]. M. Qiao, J. Fan, and X. Liu, "Federated reinforcement learning for adaptive modulation and coding in heterogeneous 5G networks," IEEE Trans. Netw. Sci. Eng., vol. 9, no. 3, pp. 1456–1470, Jun. 2022.

[19]. A Felix, S. Cammerer, S. Dörner, J. Hoydis, and S. ten Brink, "OFDM-autoencoder for end-to-end learning of communications systems," in Proc. IEEE 19th Int. Workshop Signal Process. Adv. Wireless Commun. (SPAWC), Kalamata, Greece, Jun. 2018, pp. 1–5.

[20]. 3GPP RP-213599, "Study on artificial intelligence (AI)/machine learning (ML) for NR air interface," Release 18, Dec. 2021